Chinese Physics Letters

PAPER

Emergence of High-Temperature Superconducting Phase in Pressurized $La_3Ni_2O_7$ Crystals

To cite this article: Jun Hou *et al* 2023 *Chinese Phys. Lett.* **40** 117302

Emergence of High-Temperature Superconducting Phase in Pressurized $La_3Ni_2O_7$ Crystals

Jun Hou(侯钧)[1,2†], Peng-Tao Yang(杨芃焘)[1,2†], Zi-Yi Liu(刘子儀)[1,2†], Jing-Yuan Li(李婧媛)[3†], Peng-Fei Shan(单鹏飞)[1,2], Liang Ma(马良)[1,4,5], Gang Wang(王罡)[1,2], Ning-Ning Wang(王宁宁)[1,2], Hai-Zhong Guo(郭海中)[4,5], Jian-Ping Sun(孙建平)[1,2], Yoshiya Uwatoko[6], Meng Wang(王猛)[3*], Guang-Ming Zhang(张广铭)[7*], Bo-Sen Wang(王铂森)[1,2*], and Jin-Guang Cheng(程金光)[1,2*]

[1]*Beijing National Laboratory for Condensed Matter Physics, and Institute of Physics, Chinese Academy of Sciences, Beijing 100190, China*
[2]*School of Physical Sciences, University of Chinese Academy of Sciences, Beijing 100190, China*
[3]*Center for Neutron Science and Technology, Guangdong Provincial Key Laboratory of Magnetoelectric Physics and Devices, School of Physics, Sun Yat-Sen University, Guangzhou 510275, China*
[4]*Key Laboratory of Materials Physics (Ministry of Education), School of Physics and Microelectronics, Zhengzhou University, Zhengzhou 450052, China*
[5]*Institute of Quantum Materials and Physics, Henan Academy of Sciences, Zhengzhou 450046, China*
[6]*Institute for Solid State Physics, University of Tokyo, Kashiwa, Chiba 277-8581, Japan*
[7]*State Key Laboratory for Low dimensional Quantum Physics, Department of Physics, Tsinghua University, Beijing 100084, China*

(Received 28 September 2023; accepted manuscript online 8 October 2023)

The recent report of pressure-induced structural transition and signature of superconductivity with $T_c \approx 80$ K above 14 GPa in $La_3Ni_2O_7$ crystals has garnered considerable attention. To further elaborate this discovery, we carried out comprehensive resistance measurements on $La_3Ni_2O_7$ crystals grown in an optical-image floating zone furnace under oxygen pressure (15 bar) using a diamond anvil cell (DAC) and cubic anvil cell (CAC), which employ a solid (KBr) and liquid (glycerol) pressure-transmitting medium, respectively. Sample 1 measured in the DAC exhibits a semiconducting-like behavior with large resistance at low pressures and gradually becomes metallic upon compression. At pressures $P \geqslant 13.7$ GPa we observed the appearance of a resistance drop of as much as $\sim$50% around 70 K, which evolves into a kink-like anomaly at pressures above 40 GPa and shifts to lower temperatures gradually with increasing magnetic field. These observations are consistent with the recent report mentioned above. On the other hand, sample 2 measured in the CAC retains metallic behavior in the investigated pressure range up to 15 GPa. The hump-like anomaly in resistance around $\sim$130 K at ambient pressure disappears at $P \geqslant 2$ GPa. In the pressure range of 11–15 GPa we observed the gradual development of a shoulder-like anomaly in resistance at low temperatures, which evolves into a pronounced drop of resistance of 98% below 62 K at 15 GPa, reaching a temperature-independent resistance of 20 μΩ below 20 K. Similarly, this resistance anomaly can be progressively shifted to lower temperatures by applying external magnetic fields, resembling a typical superconducting transition. Measurements on sample 3 in the CAC reproduce the resistance drop at pressures above 10 GPa and realize zero resistance below 10 K at 15 GPa even though an unusual semiconducting-like behavior is retained in the normal state. Based on these results, we constructed a dome-shaped superconducting phase diagram and discuss some issues regarding the sample-dependent behaviors on pressure-induced high-temperature superconductivity in the $La_3Ni_2O_7$ crystals.

DOI: 10.1088/0256-307X/40/11/117302

First-row (3*d*) transition-metal oxides (TMOs) with perovskite and related structures provide fertile ground for the discovery of novel emergent quantum phenomena due to their intimate interplay of spin, charge, orbital and lattice degrees of freedom.[1–3] The discovery of unconventional high-temperature superconductivity in cuprates represents one of the most celebrated examples,[4–6] and has encouraged continuous efforts to find more unconventional superconducting systems among the 3*d* TMOs. As the nearest neighbor to copper in the periodic table, nickel oxides (nickelates) have gained considerable attention since the early 1990s as the most promising candidates for high-T_c superconductivity.[7–10] However, experimental breakthroughs in this direction have not been achieved up to recent dates. In 2019, Li *et al.* successfully synthesized hole-doped infinite-layer $Nd_{1-x}Sr_xNiO_2$ thin films through

†These authors contributed equally to this work.
*Corresponding authors. Email: wangmeng5@mail.sysu.edu.cn; gmzhang@mail.tsinghua.edu.cn; bswang@iphy.ac.cn; jgcheng@iphy.ac.cn

a topotactic reduction reaction of the perovskite phase by using CaH_2 and discovered superconductivity with T_c around 9–15 K.[11–13] Such a discovery stimulated many theoretical discussions on the similarities and differences between cuprates and nickelates.[14–17] It was later found that the T_c of $Pr_{0.82}Sr_{0.18}NiO_2$ thin films can be enhanced to over 30 K at 12.1 GPa, which underscores the potential for further raising T_c of the superconducting nickelates.[18]

More recently, Sun *et al.* have reported on the signature of superconductivity with $T_c \approx 80$ K above 14 GPa in the $La_3Ni_2O_7$ crystal,[19] which is the $n = 2$ member of the Ruddlesden–Popper phase $La_{n+1}Ni_nO_{3n+1}$. Although polycrystalline $La_3Ni_2O_{7\pm\delta}$ has been well studied before, experimental studies on single-crystalline samples are rather scarce due to the difficulty in growing large single crystals.[20–23] By using the optical-image floating zone method, Liu *et al.*[24] synthesized large-sized $La_3Ni_2O_7$ single crystals under a moderate oxygen pressure $p(O_2) = 15$ bar and revealed a metallic behavior with obvious anomalies in resistivity and magnetic susceptibility at about 110 K and 153 K associated with the formation of a density-wave-like transition in this system. When these $La_3Ni_2O_7$ crystals were subjected to compression in a diamond anvil cell (DAC), Sun *et al.* observed a pressure-induced structural transition from the space group *Amam* to *Fmmm* around 14 GPa, which straightens the interlayer Ni–O–Ni bond angle within the bilayers of NiO_6 octahedra.[19] Concomitant with the structural transition, they observed the emergence of a pronounced drop in resistance around 80 K. Since this anomaly can be gradually suppressed by external magnetic fields and the ac magnetic susceptibility also shows a corresponding drop at a similar temperature, it has been attributed to the occurrence of a superconducting transition with $T_c \approx 80$ K. This discovery is exciting as it represents a second class of $3d$ TMO superconductors with T_c above the liquid-nitrogen boiling temperature of 77 K.

To reach a decisive conclusion on the occurrence of high-T_c superconductivity in $La_3Ni_2O_7$, however, some important issues have to be clarified: (i) The zero-resistance state has not yet been achieved. (ii) It remains unclear how the metallic sample at ambient pressure is altered to a semiconductor when subjected to compression in a DAC. (iii) How the density-wave-like transitions evolve with pressure and the emergent high-T_c superconductivity also needs exploration. There is no doubt that more comprehensive high-pressure (HP) studies are needed to address these issues. Previous HP studies on polycrystalline $La_3Ni_2O_7$ samples have revealed that its transport properties are sensitive to pressure conditions, i.e., hydrostatic versus non-hydrostatic pressure.[25] In this work, therefore, we carried out a comparative study on the transport properties of $La_3Ni_2O_7$ crystals using two distinct HP techniques under different pressure conditions, i.e., a DAC and a cubic anvil cell (CAC) employing a solid (KBr) and liquid (glycerol) pressure-transmitting medium (PTM), respectively. For measurements in a DAC, the results are consistent with the recent report of Sun *et al.*[19] Remarkably, measurements in a CAC under excellent hydrostatic pressure conditions have revealed distinct evolution of the metallic transport properties and the gradual development of a resistance drop in the pressure range between 11 GPa and 15 GPa, partially addressing the above-mentioned issues (ii) and (iii). Some sample-dependent issues are also revealed in the present study.

Experimental. Small pieces of $La_3Ni_2O_7$ samples used in the present work were extracted from large crystals grown in an optical-image floating zone furnace under an oxygen pressure $p(O_2) = 15$ bar at Sun Yat-Sen University in China. Details about the crystal growth and physical property characterizations at ambient pressure have been published elsewhere.[24] In the present study, we found that the electrical transport properties of the studied $La_3Ni_2O_7$ samples have strong sample-dependent issues, and the samples can be generally categorized into two groups, i.e., some display an insulating behavior over the entire temperature range while others exhibit a metallic behavior with a weak hump-like anomaly in resistance around 110–130 K. Such observations of distinct, sample-dependent transport behaviors should be attributed to the different oxygen stoichiometries in the studied samples. According to previous studies on polycrystalline $La_3Ni_2O_{7-\delta}$, its transport properties can change significantly from metallic to insulating behavior for δ as small as 0.08.[20,22] It is thus plausible that the as-grown $La_3Ni_2O_7$ crystals have a non-uniform distribution of oxygen concentration. In addition to the chemical inhomogeneity, the oxygen stoichiometry of $La_3Ni_2O_7$ crystals may also be modified during the post-handling process. We found that the contact resistance of some $La_3Ni_2O_7$ crystals increases when the electrical leads were directly attached to the sample surface using sliver paste (DuPont 4929N). To prevent direct contact of silver paste with the sample surface, we deposited four platinum (Pt) pads with a magnetron sputtering machine and then attached the gold wires to these Pt pads using silver paste.

We performed HP resistance measurements on three $La_3Ni_2O_7$ samples using a DAC (sample 1) and a CAC (samples 2 and 3). For measurements in the DAC, sample 1 [inset of Fig. 1(a)] was loaded into a pre-indented gasket hole filled with KBr as the solid PTM in between a pair of diamond anvils with a 300 μm culet. Four gold leads were manually put on the sample surface and the electrical contact maintained by mechanical compression. A piece of ruby ball placed near the sample in the DAC is used as the pressure calibrant and the pressure is determined by monitoring the position of the ruby fluorescence R1 line at room temperature. For samples 2 and 3, we employed a palm-type CAC for resistance measurements up to 15 GPa using a standard four-probe method. Sample 2 has dimensions of 0.60 mm × 0.21 mm × 0.06 mm and sample 3 is of 0.52 mm × 0.16 mm × 0.09 mm. As seen in Fig. 2(a), the sample is hung inside a Teflon capsule filled with glycerol as the liquid PTM. As shown in our previous work, the three-axis compression geometry together with the adoption of a liquid PTM ensures excellent hydrostatic pres-

sure conditions in the CAC up to 15 GPa.[26] The pressure values inside the CAC were estimated from the pressure-loading force calibration curve pre-determined by measuring the structural phase transitions of Bi, Sn and Pb at room temperature. All low-temperature experiments were carried out in a ^{4}He refrigerated cryostat equipped with a 9 T superconducting magnet.

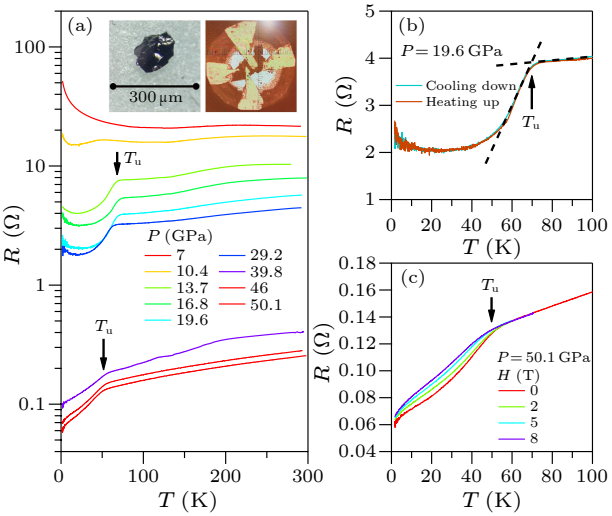

Fig. 1. (a) Temperature-dependent resistance $R(T)$ of $La_3Ni_2O_7$ crystal (sample 1) under various pressures up to 50.1 GPa measured in a DAC employing KBr as the solid pressure-transmitting medium. The inset shows images of the crystal at ambient pressure and in the DAC. (b) An enlarged view of $R(T)$ at 19.6 GPa below 100 K recorded upon warming-up and cooling-down processes. (c) $R(T)$ curves at 50.1 GPa under different magnetic fields from 0 to 8 T.

Results and Discussion—High-Pressure Resistance Measurements on Sample 1 in a DAC. Figure 1(a) shows the temperature-dependent resistance $R(T)$ in a semi-logarithmic scale for sample 1 measured in a DAC under various pressures up to 50.1 GPa. Because this sample is very small, we did not measure its $R(T)$ at ambient pressure. At the first applied pressure of 7 GPa in the DAC, $R(T)$ exhibits a weakly insulating behavior upon cooling down with a room-temperature value of about 25 Ω. The metallic behavior at ambient pressure is completely altered upon compression in the DAC. Similar observations have also been reported in the literature.[19] When the pressure is increased to 10.4 GPa, $R(T)$ decreases in the whole temperature range, exhibits a weaker temperature dependence at high temperatures and then displays a downturn at about 40 K followed by a slight upturn at lower temperatures. Upon further increasing the pressure to 13.7 GPa, a metallic behavior is realized in $R(T)$ at high temperatures, and a clear drop of resistance of 50% appears at about 70 K, which is close to but slightly lower than that of T_c defined as the superconducting transition temperature in Ref. [19].

As in the previous report,[19] a finite value of resistance is preserved below the transition and $R(T)$ even goes up again at temperatures below 20 K. Thus, we define the transition temperature as T_u from the intercept of two straight lines across the resistance anomaly as illustrated in Fig. 1(b). No thermal hysteresis is observed around this anomaly, as shown in Fig. 1(b). Similar $R(T)$ behaviors are observed at pressures up to 29.2 GPa, and the transition temperature T_u first increases slightly to 70.7 K at 16.8 GPa and then decreases gradually to 63 K with increasing pressure to 29.2 GPa. When the pressure is increased from 29.2 GPa to 39.8 GPa, the room-temperature resistance decreases suddenly by nearly one order of magnitude from ∼4 Ω to 0.4 Ω, and $R(T)$ exhibits a strong temperature dependence in the whole temperature range. Meanwhile, the low-temperature upturn disappears and the drop anomaly at T_u is replaced by a kink-like anomaly in $R(T)$, and T_u is suppressed to about 50 K at 50 GPa. At the highest pressure of 50.1 GPa, we also measured $R(T)$ under different external magnetic fields displayed in Fig. 1(c), which shows a gradual suppression of the resistance below T_u, reminiscent of the observations in Ref. [19]. Overall, the above results are consistent with those reported results,[19] showing a pronounced drop or kink-like anomaly in resistance at $T_u \approx 70$ K under pressures above ∼13 GPa. Due to the absence of zero resistance for the above data in the DAC, however, it was ascribed to a signature of superconducting transition at this stage.

High-Pressure Resistance Measurements on Sample 2 in a CAC. At ambient pressure, $La_3Ni_2O_7$ crystal shows a metallic behavior with a density-wave-like transition at $T_s \approx 110$–150 K, which is manifested as obvious anomalies in $R(T)$. For the polycrystalline samples, the temperature-dependent $R(T)$ changes from metallic above T_s to a semiconducting-like behavior below T_s.[27] In contrast, the measured $R(T)$ of $La_3Ni_2O_7$ single crystals presents a weaker hump-like anomaly at T_s and remains metallic below T_s down to the lowest temperature. Previous HP studies on the transport properties of $La_3Ni_2O_7$ polycrystalline samples have shown that both resistance and T_s decrease monotonically with pressure below 2 GPa with a slope of $dT_s/dP = 10.7$–$12.5\ \mathrm{K{\cdot}GPa^{-1}}$, which would predict a complete suppression of T_s at ∼10 GPa.[25] For the above HP resistance measurements in the DAC, the metallic behavior has unfortunately been altered by the non-hydrostatic pressure conditions, thus preventing us from observing intrinsic evolution of the transport properties under HP. To overcome this problem, we resorted to the CAC technique, which employs a three-axis compression geometry and adopts a liquid PTM to maintain excellent hydrostatic pressure conditions up to 15 GPa.

Figure 2(a) shows the obtained $R(T)$ data for sample 2 under various pressures up to 15 GPa in the CAC. At ambient pressure, $R(T)$ displays a metallic behavior over the whole temperature range with a weak hump-like anomaly at $T_s = 136$ K, which can be determined from the peak position of dR/dT. In comparison with the previous report showing residual resistivity ratio RRR = 2.5, the present sample exhibits a larger RRR of 15, signaling a better-quality sample. The room-temperature resistivity value is estimated to be ∼18 mΩ·cm. As seen in Fig. 2(a),

the metallic behavior of $R(T)$ is retained upon compression in the CAC, strikingly different from the above results in the DAC, and the magnitude of resistance decreases monotonically with increasing pressure, especially in the high-temperature region. At the first applied pressure of 2 GPa, the hump-like anomaly in $R(T)$ can no longer be discerned, suggesting complete suppression of the density-wave-like transition by pressure. To track the evolution of $T_s(P)$ in the low-pressure range, HP resistance measurements using a piston-cylinder cell are in progress.

For pressures between 2 GPa and 9 GPa, the $R(T)$ curves show a plain metallic behavior without any discernible anomaly down to 1.5 K. Upon further increasing the pressure to 11 GPa, we observed a slight upturn in $R(T)$ below 10 K followed by a faint drop below 5 K, which even shows some field dependence. This feature motivated us to measure $R(T)$ in a finer pressure interval between 11 and 15 GPa. As seen in Fig. 2(b), the measured $R(T)$ at 12 GPa exhibits a weak kink around 25 K and then develops a broad shoulder centered around 10 K, which can be eliminated by external magnetic fields (see Fig. S1 in the Supplementary Information). These features become more pronounced and move to higher temperatures with increasing pressure, and the shoulder feature also fades away gradually. Finally, the resistance $R(T)$ at 15 GPa is characterized by quite a sharp drop at $T_0 \approx 62$ K followed by a long tail between ~ 48 K and 20 K and then a nearly temperature-independent resistance of 20 μΩ below 20 K. This value is about 2% of the resistance at T_0, i.e., the resistance drops by 98% from T_0 to the lowest temperature of 1.5 K. Such a large drop in resistance with a nearly temperature-invariant $R(T)$ over a wide temperature range is unlikely to be caused by magnetic or electronic phase transitions but is more probably associated with the occurrence of a superconducting transition. The presence of a small residual resistance together with the observation of a relatively wide transition indicates that the volume ratio of the possible superconducting phase is low at this pressure. Indeed, measurements of ac magnetic susceptibility up to 15 GPa in the CAC fail to detect any superconducting shielding effect, in accordance with the resistance results. Upon decompression from 15 GPa, the recovered $La_3Ni_2O_7$ sample remained intact and its $R(T)$ was measured again at ambient pressure. As shown in Fig. 2(a), the obtained $R(T)$ is almost identical to the initial curve before compression. This result confirms that the pressure-induced changes are reversible at least up to 15 GPa in the CAC.

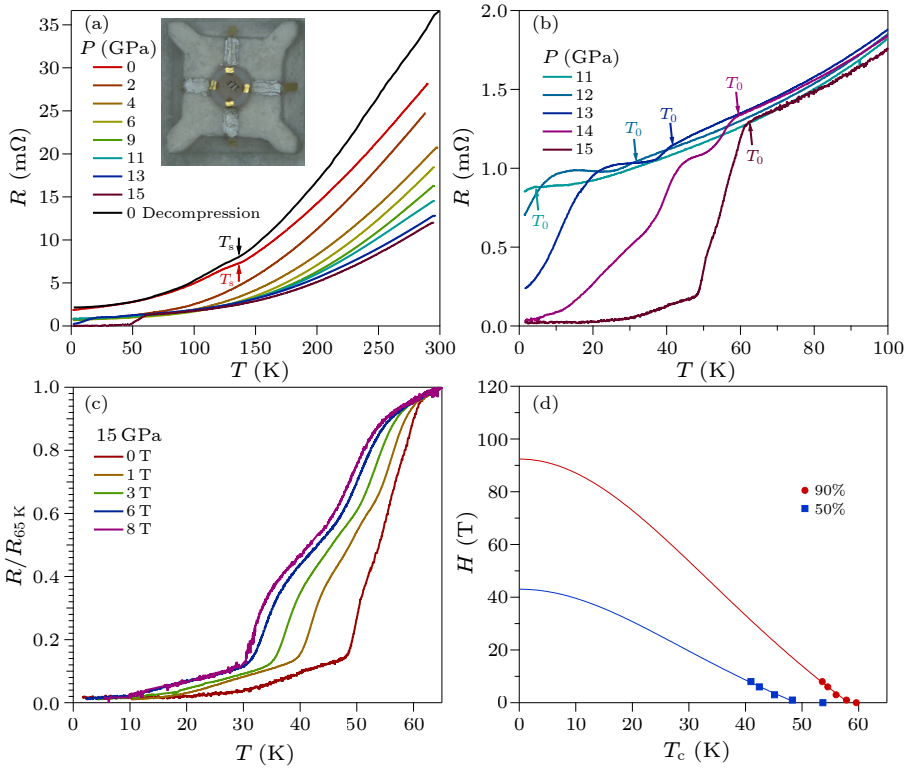

Fig. 2. (a) Temperature-dependent resistance $R(T)$ of $La_3Ni_2O_7$ (sample 2) crystal under various hydrostatic pressures up to 15 GPa measured in a CAC employing glycerol as the liquid pressure-transmitting medium. (b) Enlarged view of low-temperature $R(T)$ data at pressures between 11 and 15 GPa, highlighting the gradual development of the resistance drop upon compression. (c) The normalized low-temperature $R(T)/R(65\,\text{K})$ at 15 GPa under different magnetic fields. (d) The temperature dependence of $\mu_0 H_{c2}(T)$ fitted by the Ginzburg–Landau equation.

To check whether the observed resistance drop is truly associated with a superconducting transition, we measured $R(T)$ at 15 GPa under different magnetic fields. Figure 2(c) shows the normalized $R(T)$ below 65 K. As can be seen, the transition gradually shifts to lower temperatures with increasing magnetic field, similar to a super-

conducting transition. Thus, we tentatively ascribed the observed resistance drop to the onset of superconducting transition, i.e., $T_0 = T_c^{onset}$. Here we define $T_c^{90\%}$ and $T_c^{50\%}$ at each field according to the criteria of 90% and 50% of the corresponding normal-state resistance at T_c^{onset}, and then plot the temperature dependence of $\mu_0 H_{c2}(T_c)$ in Fig. 2(d). Least-squares fitting to these data using the empirical Ginzburg–Landau equation yields the zero-temperature upper critical field $\mu_0 H_{c2}(0) = 92$ T and 43 T for $T_c^{90\%}$ and $T_c^{50\%}$, respectively.

High-Pressure Resistance Measurements on Sample 3 in the CAC. To check the reproducibility of the observed resistance drop in sample 2, we loaded another sample 3 into the CAC for resistance measurements at high pressures. As seen in Fig. 3(a), this sample shows a metallic behavior over the entire temperature range at ambient pressure, with an obvious anomaly at about $T_s \approx 110$ K in $R(T)$. The metallic behavior can be retained at 2 GPa, but changes to semiconducting behavior at 10 GPa, which is different from the results for sample 2 [see Fig. 2(a)].

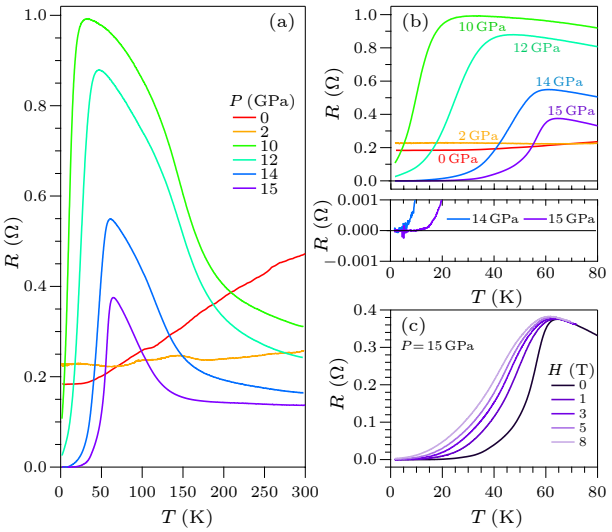

Fig. 3. (a) Temperature-dependent resistance $R(T)$ of $La_3Ni_2O_7$ crystal (sample 3) under various hydrostatic pressures up to 15 GPa measured in a CAC employing glycerol as the liquid pressure-transmitting medium. (b) Enlarged view of the low-temperature $R(T)$ data. (c) The low-temperature resistivity $R(T)$ at 15 GPa under different magnetic fields.

As can be seen, the measured $R(T)$ at 10 GPa first increases upon cooling down, with an obvious slope change around 150 K, and then drops suddenly below ~20 K. At this pressure the resistance drops by 90% at 1.5 K and the applied magnetic fields can suppress this drop, signaling the occurrence of a superconducting transition. With increasing pressure from 10 GPa to 12 GPa, 14 GPa, and 15 GPa, the resistance in the normal state retains a similar feature but the magnitude decreases progressively, while the drop in resistance moves quickly to higher temperatures, with the onset temperature increasing to ~42 K, 60 K, and 64 K at 12 GPa, 14 GPa, and 15 GPa, respectively. Interestingly, the resistance $R(T)$ at 14 GPa and 15 GPa can finally reach zero below about 5 K and 10 K [see the lower panel of Fig. 3(b)], confirming the occurrence of superconductivity. However, the observation of such a broad transition indicates that the superconducting volume fraction is still low at this pressure. As shown in Fig. 3(c), the field dependence of $R(T)$ is also consistent with a superconducting transition.

The characteristic temperatures T_s, T_u, and T_0 defined in the above DAC and CAC resistance measurements as a function of pressure are summarized in Fig. 4. The T_c values determined from the measurements in a DAC in Ref. [19] are also included for comparison. As can be seen, the $T_u(P)$ determined in the present work matches well with the value of $T_c(P)$ in the previous work, and $T_0(P)$ connects rather smoothly to $T_c(P)$, implying a common origin for these anomalies in resistance. Importantly, our results together with the previous study reveal a dome-shaped superconducting phase in the pressurized $La_3Ni_2O_7$ crystals. Whether it is associated with the proposed structural phase transition or adjacent to other electronic phases deserves further experimental investigations.

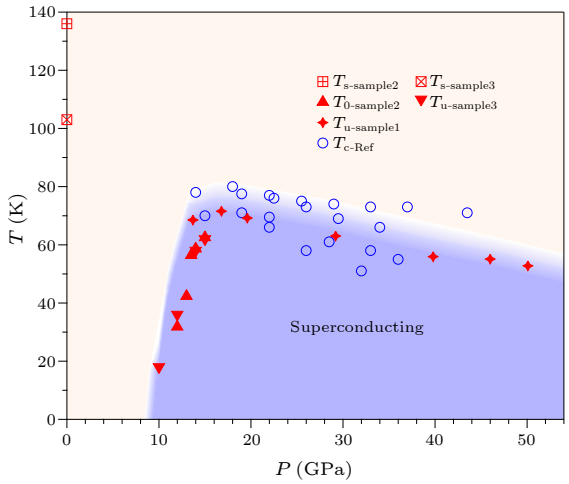

Fig. 4. The temperature–pressure (T–P) phase diagram of $La_3Ni_2O_7$ crystal. The red squares represent the density-wave-like transition T_s measured at ambient pressure. The red filled triangles and stars represent the onset superconducting temperatures determined from the present measurements in a CAC and DAC, respectively. The blue circles are taken from Ref. [19].

Through the above detailed resistance measurements in a CAC, we have revealed the emergence and gradual development of a possible superconducting phase above 10–11 GPa, and its volume seems to increase gradually with pressure but retains a filamentary nature up to 15 GPa. This may be related to the nature of a first-order structure transition around 15 GPa from the low-pressure phase (space group *Amam*) to the HP phase (space group *Fmmm*), as reported in the recent experiments.[19] Usually, the coexistent phases appear in the first-order transition and span a finite region in the phase diagram. More studies are definitely needed to check whether the bulk superconducting state can be eventually achieved at a higher pressure in $La_3Ni_2O_7$. In this regard, a two-stage multi-

anvil press that can reach hydrostatic pressures up to 20 GPa would be valuable for this purpose. Nonetheless, the present study provides detailed information about the emergence and evolution of a superconducting phase in $La_3Ni_2O_7$ crystal in the critical pressure regime.

The Sample-Dependent Issues. In the present study, we have provided more evidence in support of the emergence of a high-T_c superconducting phase above ~ 10 GPa in $La_3Ni_2O_7$ crystals grown under a moderate oxygen pressure of 15 bar. As mentioned above, however, our results also suggest strong sample-dependent issues besides sensitivity to the pressure environments. Samples 2 and 3 measured in the CAC both show a metallic behavior with a weak hump-like anomaly in $R(T)$ at ambient pressure, but their values of T_s (136 K and 103 K) are slightly different. In addition, sample 3 possesses a much-reduced RRR of 2.5 and its room-temperature resistance is about one order higher than that of sample 2, as shown in Fig. 2(a). These differences may be responsible for the observed distinct responses of resistance to pressure at high temperatures. Under high pressures, sample 2 retains a metallic behavior up to 15 GPa, while sample 3 changes to semiconducting behavior. Since the pressure conditions are the same, the observed distinct responses to the applied pressure should be caused mainly by sample-dependent issues.

To characterize these samples, we performed scanning electron microscopy with energy dispersive x-ray spectroscopy measurements on sample 2 (after decompression) and some samples from the same batch as sample 3. The results are summarized in Figs. S2 and S3 in the Supplementary Information. As can be seen, all samples show some variations in chemical composition, with the La : Ni ratio varying in micrometer-sized regions. For sample 2, we checked several points and observed some regions with a La : Ni ratio close to 3 : 2 coexisting with some Ni-rich/La-deficient regions, which are also observed on the samples shown in Figs. S3(b)–S3(d). The presence of these Ni-rich/La-deficient regions can rationalize the observed deviations of the La : Ni ratio from the stoichiometric 3 : 2. According to a previous study,[28] the formation of Ruddlesden–Popper phases $La_{n+1}Ni_nO_{3n+1}$ depends sensitively on the oxygen pressure, and the $La_3Ni_2O_7$ crystal can only be prepared within a narrow oxygen pressure range between 10 and 18 bar. Some La_2NiO_4 phase was observed in the x-ray diffraction pattern of $La_3Ni_2O_7$ crystal grown under 15 bar oxygen pressure in Ref. [28]. Given the starting composition of $La_3Ni_2O_7$, we would expect to have some NiO secondary phase in the presence of La_2NiO_4. This may explain the observed Ni-rich regions. In addition, the oxygen content is another important factor that can influence the physical properties of oxides. Whether these enclosures and the variation in oxygen content could influence the physical properties deserves further investigations, and more detailed studies on the samples with well-controlled quality are needed to finally resolve these issues.

In summary, we have employed a palm-type CAC apparatus to measure the HP resistance of $La_3Ni_2O_7$ crystals up to 15 GPa. Under hydrostatic pressure conditions, our results confirm the emergence of a high-T_c superconducting phase in $R(T)$ at a pressure above 10–11 GPa, and the onset temperature can reach about 62 K at 15 GPa. Together with the present and previous results in a DAC, our study reveals a dome-shaped superconducting phase in the pressurized $La_3Ni_2O_7$ crystals.

Acknowledgements. This work was supported by the Beijing Natural Science Foundation (Grant No. Z190008), the National Key Research and Development Program of China (Grant Nos. 2018YFA0305700 and 2021YFA1400200), the National Natural Science Foundation of China (Grant Nos. 12025408, 11921004, 11834016, and 11888101), the Strategic Priority Research Program of CAS (Grant No. XDB33000000), CAS Project for Young Scientists in Basic Research (Grant Nos. 2022YSBR-047 and 2022YSBR-048), and the Users with Excellence Program of Hefei Science Center CAS (Grant No. 2021HSCUE008). Work at Sun Yat-Sen University was supported by the National Natural Science Foundation of China (Grant No. 12174454), Guangdong Basic and Applied Basic Research Funds (Grant No. 2021B1515120015), and Guangdong Provincial Key Laboratory of Magnetoelectric Physics and Devices (Grant No. 2022B1212010008). The high-pressure experiments were performed at the Cubic Anvil Cell Station of Synergic Extreme Condition User Facility (SECUF).

References

[1] Adler D 1968 *Rev. Mod. Phys.* **40** 714
[2] Imada M, Fujimori A, and Tokura Y 1998 *Rev. Mod. Phys.* **70** 1039
[3] Bednorz J G and Muller K A 1986 *Z. Physik B* **64** 189
[4] Anderson P W 1987 *Science* **235** 1196
[5] Lee P A *et al.* 2006 *Rev. Mod. Phys.* **78** 17
[6] Keimer B *et al.* 2015 *Nature* **518** 179
[7] Hayward M A *et al.* 1999 *J. Am. Chem. Soc.* **121** 8843
[8] Boris A V *et al.* 2011 *Science* **332** 937
[9] Disa A S *et al.* 2015 *Phys. Rev. Lett.* **114** 026801
[10] Nakata M *et al.* 2017 *Phys. Rev. B* **95** 214509
[11] Li D F *et al.* 2019 *Nature* **572** 624
[12] Osada M *et al.* 2020 *Phys. Rev. Mater.* **4** 121801
[13] Pan G A *et al.* 2022 *Nat. Mater.* **21** 160
[14] Lee K W and Pickett W E 2004 *Phys. Rev. B* **70** 165109
[15] Sakakibara H *et al.* 2020 *Phys. Rev. Lett.* **125** 077003
[16] Botana A S and Norman M R 2020 *Phys. Rev. X* **10** 011024
[17] Zhang G M, Yang Y F, and Zhang F C 2020 *Phys. Rev. B* **101** 020501
[18] Wang N N *et al.* 2022 *Nat. Commun.* **13** 4367
[19] Sun H *et al.* 2023 *Nature* **621** 493
[20] Zhang Z, Greenblatt M, and Goodenough J B 1994 *J. Solid State Chem.* **108** 402
[21] Yoshiaki K *et al.* 1996 *J. Phys. Soc. Jpn.* **65** 3978
[22] Taniguchi S *et al.* 1995 *J. Phys. Soc. Jpn.* **64** 1644
[23] Greenblatt M *et al.* 2007 *Synth. Met.* **85** 1451
[24] Liu Z J *et al.* 2023 *Sci. China Phys. Mech. Astron.* **66** 217411
[25] Hosoya T *et al.* 2008 *J. Phys.: Conf. Ser.* **121** 052013
[26] Cheng J G *et al.* 2018 *Chin. Phys. B* **27** 077403
[27] Wu G Q *et al.* 2001 *Phys. Rev. B* **63** 245120
[28] Zhang J J *et al.* 2020 *Phys. Rev. Mater.* **4** 083402